Springer

KSME

Journal of Mechanical Science and Technology 25 (7) (2011) 1767~1774
www.springerlink.com/content/1738-494x
DOI 10.1007/s10.1007/s12206-011-0507-8

Wind pressure distribution on canopies attached to tall buildings †

Hyung-Woon Roh[1] and Ha-Rim Kim[2,*]
[1]*President, IVAIGD3, Seoul, 157-861, Korea*
[2]*Architectural Engineering, Juseong University, Cheongwon-Kun, Chungbuk 363-794, Korea*

(Manuscript Received October 19, 2010; Revised April 5, 2011; Accepted April 5, 2011)

Abstract

This paper presents the numerical simulations of wind pressure distributions on canopies attached to tall and medium-rise buildings. The most current wind pressure coefficients in wind load codes do not take into account the large scale canopies attached to tall and medium-rise L-shaped buildings. Wind pressure on canopies attached to buildings depends on the building geometry and its features, the location of canopies, surrounding buildings and terrain, as well as canopy sizes and wind directions. Numerical analysis results were compared and investigated using ANSYS CFX 11 codes. Numerical simulation of wind loading on a canopy attached near the base of a tall or medium-height L-shaped building has shown that the downward pressure on the canopy does not grow in proportion to the increase in the height of building-to-canopy ratio. As a result, the downward pressure acting on a canopy attached to a tall L-shaped building is considerably smaller than that of prismatic models used in other researches and we assume that this is due to the shape of the building itself. The results of numerical simulations of L-shaped models differ considerably from those of previous wind tunnel prismatic shape model tests.

Keywords: Canopies attached to the building; Canopies; Tall building; Pressure distributions; Numerical simulation; Flow phenomena

1. Introduction

The effects of wind on a building and its surrounding area are, in general, evaluated by measuring wind loading in wind tunnel test or by the computational fluid dynamics (CFD).

Combination members, both plate-like and bluff elements, of a building are attached to the building frame and form its structural part. These combination members include parapets around buildings, canopies and other plate-like appurtenances such as balconies and ribs.

The size of canopies situated near a building's main entrance can vary greatly depending on its design and this can make it difficult to determine wind pressure distribution on them. Furthermore, no guidelines exist for designing canopies attached to buildings in any codes of practice or standards and this can compound problems of designing canopies further.

The wind loading effects on canopies attached to a building can be classified into two groups: (a) Canopies attached near the top, or at least more than half-way up the building: (b) Canopies attached near the bottom, or at least less than half-way up the building.

† This paper was recommended for publication in revised form by Associate Editor Yang Na

* Corresponding author. Tel.: +82 43 210 8376, Fax.: +82 2 2093 2122
E-mail address: mileage@nate.com

In general, 1:400 to 1:500 building models are used in wind tunnel tests and as average canopy is 1-2 meters thick, the thickness of canopies of the model building should lie in the region of 2-4 mm. However, it is not practical to attach pressure taps on both top and bottom surfaces of a model canopy of such thickness. To be able to install the pressure taps successfully, the thickness of a model canopy needs to be at least 6-8 mm, which is approximately equivalent to height of 1 story. In order to overcome limitations imposed upon wind tunnel tests, numerical simulation techniques are often employed to complement the wind tunnel test results.

Most research in wind loading on canopies attached to buildings to date has been mainly for either roof canopies attached to tall buildings or for canopies attached to low-rise buildings. Wind loads on roof canopies received much attention in recent years [1-3], and several Japanese researchers have studied the wind loads on pitched roofs of low-rise buildings [4]. In addition, there have been several studies on the fluctuating wind forces acting on canopies attached to eaves of a low-rise building with a gable roof. Wind loads on single story buildings with gable roof and attached canopies were also investigated [5]. Wind loads on canopies attached to a building depend on the position of the canopy and configuration of building. Characteristics of fluctuating net uplift force acting on a canopy depend on the ratio of its height to its projected length [1].

To date, limited information is available regarding wind pressures acting on canopies attached to the bases of tall or medium-rise buildings.

Recently, another study showed that wind pressure distribution on a canopy varied substantially according to its location. Cho et al. examined wind pressure distributions on canopies set at various heights and pitch angles in an 11-story building [7, 8]. Some research has been conducted to investigate wind loads on canopies at the base of tall buildings. Jancauskas and Eddleston [9] confirmed through experimental measurements that the two cases to be considered in the design are a canopy on windward face for maximum downward load and a canopy on the side face for maximum upward load.

The purpose of this study is to investigate the wind effects on canopies attached near the base of tall and medium-rise buildings. This study also investigates the wind pressure coefficients on upper and lower surface of canopy models. The effects of building height-to-canopy height ratios, wind directions, and general features of the canopy sizes are determined by numerical simulation method. The analysis is extended to predict the pressure coefficients of buildings to be constructed.

2. Numerical simulations techniques

2.1 Governing equation

In this paper, a commercial Navier-Stokes code ANSYS-CFX11 is used for the turbulent flow simulations to obtain physically more accurate solutions. The following continuity and momentum equations are used in tensor form to solve the flow characteristics:

$$\nabla \cdot (\rho U) \tag{1}$$

$$\nabla \cdot (\rho U \otimes U) = -\nabla p + \nabla \cdot \tau \tag{2}$$

where ρ, U, p and τ are the density, velocity vector, pressure and stress tensor respectively. The stress tensor τ is related to the strain rate as shown in Eq. (3).

$$\tau = \mu \left[\left(\nabla U + (\nabla U) \right)^T - \frac{2}{3} \delta \nabla \cdot U \right] \tag{3}$$

One of the most important features of ANSYS CFX is its use of a coupled solver, in which all the hydrodynamic equations are solved as a single system. The coupled solver is faster than the traditional segregated solver and less iteration is required to obtain a converged flow solution. A standard k- ε turbulence model was used in this research. The code includes several alternative turbulence models, such as standard k-ε, RNG k-ε, and LES models, etc. Although it has been known that there is a deficiency in the performance of k-ε turbulence model for the problems involving the vortex and curvature, in the present paper, ANSYS-CFX11 with standard k-ε turbulence model is still used for the turbulent flow calculations, due to its robustness in practical applications. In order to stabilize a numerical solution and assure a high numerical accuracy, the high resolution scheme is used in the present calculations. The high resolution advection scheme has the desirable property of giving 2nd order accurate gradient resolution while keeping solution variables physically bounded.

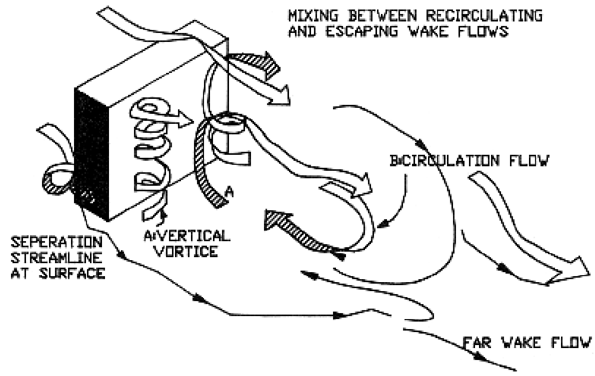

(a) Prismatic shape model

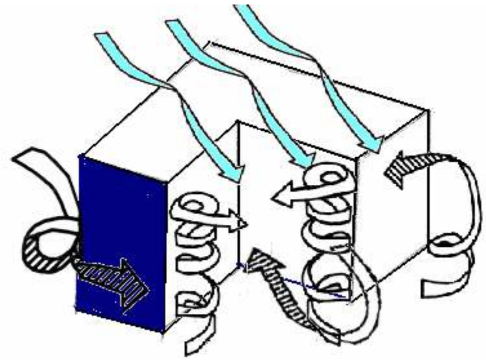

(b) L-Shaped model

Fig. 1. Plan view of flows between prismatic model and L-shaped model.

For simulation, IBM PC is used taking about 55,000s to compute the wind flows and wind pressure on each model. Total Number of Nodes and element of building with building height 48m and size of canopy is 12×12 is 76,298 and 361,058, respectively.

2.2 Model description

The characteristics of wind loadings on prismatic model shapes are already well documented through both wind tunnel experiments and numerical simulations as shown in Fig. 1(a) [11]. It indicates general occurence of mixing between recirculating and escaping wake flow, the vertical vortex, circulation flow and the far wake flow in the rear region and the streamline separation at side surface.

However, the more complex building shapes that include projections or recesses superimposed on a basic rectangular plan produce their own specific wind pattern, more complicated than that of a prismatic building. Thus, some generalizations can be made to illustrate the principal flow features that

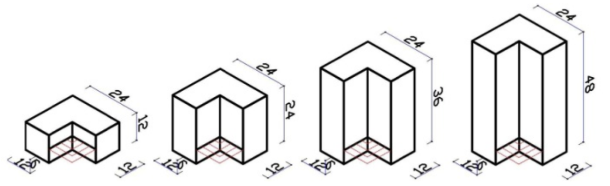

Fig. 2. Canopy attached buildings of different height.

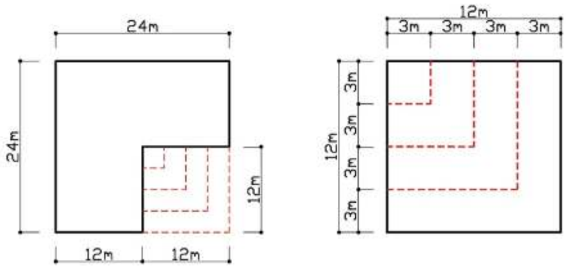

Fig. 3. Plan view of a model building with different canopy sizes.

result from such building shapes. Consider a case of a simple L-shaped building as in Fig. 1(b).

When wind blows against a major face as shown above, the air stream is diverted round the building as shown in Fig. 1(b). It is then drawn into a large eddy formed at the recessed corners, from which it escapes partly downwind, but also by spiraling upward, where it joins the flow over the roof. From Kim et al.'s results, wind pressure distribution is not appreciably more severe than for the plain rectangle model but the eddy will produce reverse flow on part of the apparently sheltered wall and an appreciation of this effect is of value in planning the arrangement of entrance doorways.

In order to investigate the effects of building geometries and features of the wind pressure coefficients, in all cases, model conditions were kept constant as follows; Exposure category C, 30 m/s basic wind speed, means wind velocity at a height is equal to that of the top of the model building, canopy attached 6 m above ground, L-shaped model with recessed 12 m by 12 m square from 24 m by 24 m square model as like Fig. 2. Given above mentioned conditions, a total of 48 types of model parameters are considered in this study.

Fig. 2 shows four different building heights with same canopy height. The ratios of building height-to-canopy height used in this study are 2:1, 4:1, 6:1 and 8:1. Fig. 3 also shows a plan view of the model building and four different sizes of canopies attached to the wall. Fig. 4 explains the definition of three different types of wind directions; direction 1 indicates front recessed face of model building while directions 2 and 3 refer to plan view of a side surface and plan view of rear surface, respectively.

The most important characteristic of this model building is its flow phenomenon around the canopies. This study also investigates the effects of the wind direction changes, the canopy size, ratios of building height-to-canopy height using computational fluid dynamic as shown in Table 1 below.

Table 1. Main parameters of model building.

Main parameter	Variations	Types	Remark
building height	12 m, 24 m, 36 m, 48 m	4 Types	Fig. 2
size of canopy	3×3, 6×6, 9×9, 12×12	4 Types	Fig. 3
wind direction	Front, Side, Rear	3 Types	Fig. 4

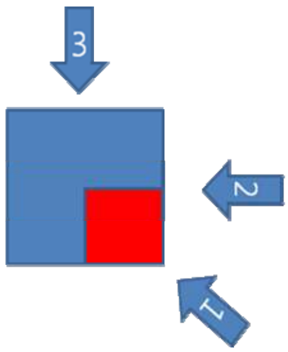

Fig. 4. Definition of wind direction 1, 2 and 3.

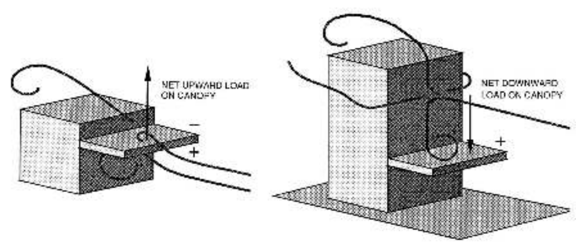

(a) Low H/hc (b) High H/hc

Fig. 5. Defined the wind loading concepts of attached canopies by Jancauskas and Holms [1].

2.3 Parameter notation

C_p, C_f, H and hc refer to pressure coefficient, net pressure coefficient of canopy, building height and canopy height above ground, respectively. In numerical simulation, all upper and lower canopy surface pressure coefficients are expressed as signed numbers followed by actual wind loading directions. The sign of a surface pressure coefficient is determined by whether the wind loading on the surface is pushing(+) or pulling(-). Net pressure coefficients are shown as unsigned numbers followed by clear indication of the direction of net wind loading.

As shown in Fig. 5, Jancauskas and Holms [1] defined the concept of exposed pressure coefficient in the canopy to the longitudinal flow; this result in the development of negative pressure on at least part of the upper surface of the canopy, together with the positive pressure developed underneath the canopy, produces a net upward force. However, as the building becomes taller, the loading mechanism for canopies mounted on the windward face of the building changes. Jan-

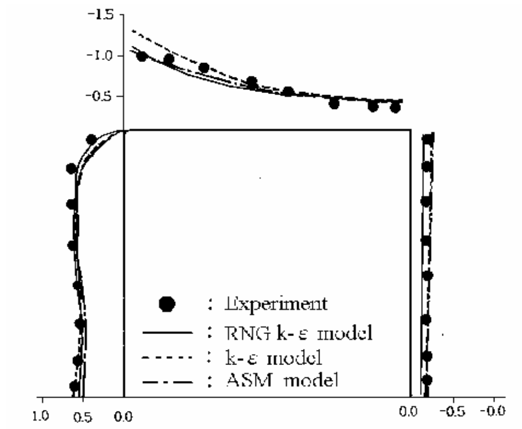

Fig. 6. Comparison of experimental data and Numerical simulation.

causkas and Holms shown that for a canopy mounted on the windward face if a tall building the dominant net load on the canopy will be downward.

3. Results and discussion

3.1. Verification of numerical simulation

In order to verify the validation of numerical simulation, it was compared with numerical results and experimental results [12] around the prismatic shape model. It can be analyzed with various turbulence models as shown in Fig. 6. Standard k-ε, RNG k-ε, and ASM models were applied. The calculated results are in good agreement with experimental data quantitatively. Among all the turbulence models, the k-ε model results are especially close to the experimental ones. The average wind pressure coefficient of the front is 0.48 and that of the roof and rear surface is -0.44 and -0.17, respectively. In this case, the wind pressure coefficients on the roof and side wall surface show rapid decrease in the back.

3.2. Effects of various building height ratio

3.2.1 Front wind direction case (arrow 1)

Numerical simulation showed that when *H/hc*=2, the pressure coefficients for lower and upper surfaces of canopies are approximately +1.4 and +0.1~+0.4 respectively regardless of the canopy size, and therefore the net uplift coefficients lie within the range of 1.0~1.3 as shown in Table 2 and Fig. 7(a) and Fig. 8. And Table 2, 3, 4 and 5 describe the results of local and net pressure coefficient on the various models using numerical simulation.

This result is mainly due to the strong wind pressure acting on the lower surface of the canopy and it is in good agreement with many of the previous studies. When *H/hc*=4, the uplift pressure coefficient for the lower surface of 3 m×3 m canopy is +1.4, while the pressure coefficients of other 3 canopies are in the region of +1.2 as the Table 3.

Downward pressure coefficients are very similar to the

Table 2. Cp, C_f results from numerical simulation for the H/hc=2.

Canopy Size		Wind Direction		
		Front	Side	Rear
3×3	upper	1.420	0.457	-0.480
	lower	1.440	0.551	-0.391
	net	-0.020	-0.094	-0.089
6×6	upper	1.121	0.469	-0.576
	lower	1.153	0.587	-0.437
	net	-0.032	-0.118	-0.139
9×9	upper	1.071	0.469	-0.517
	lower	1.142	0.654	-0.419
	net	-0.072	-0.186	-0.098
12×12	upper	0.979	0.336	-0.569
	lower	1.108	0.612	-0.410
	net	-0.129	-0.276	-0.158

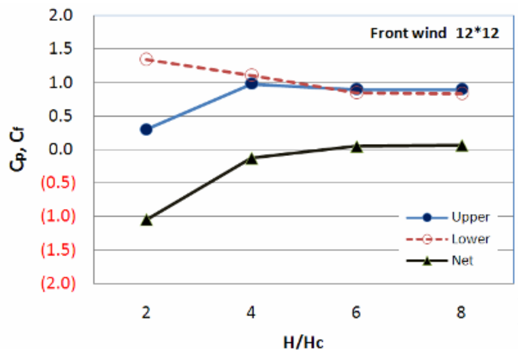

(a) Front wind direction

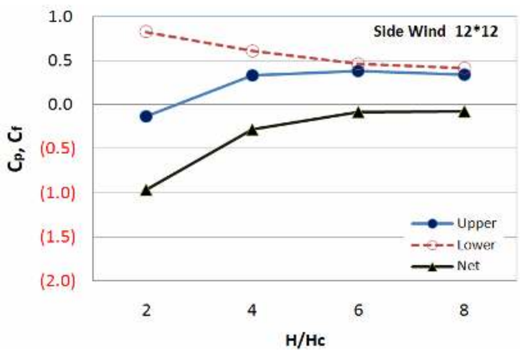

(b) Side wind direction

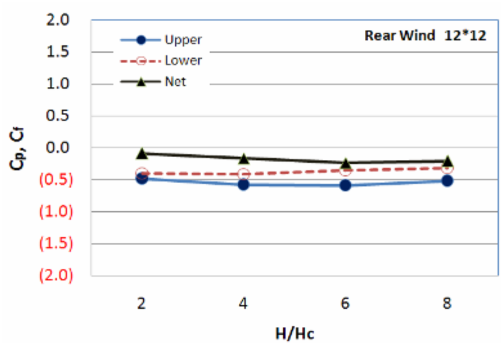

(c) Rear wind direction

Fig. 7. Canopy load as a function of H/hc (Canopy size 12 m×12 m).

Table 3. *Cp*, C_f results from numerical simulation for the H/hc=4.

Canopy Size		Wind Direction		
		Front	Side	Rear
3×3	upper	0.429	-0.111	-0.675
	lower	1.375	0.398	-0.492
	net	-0.946	-0.509	-0.183
6×6	upper	0.141	-0.182	-0.471
	lower	1.393	0.574	-0.435
	net	-1.252	-0.757	-0.036
9×9	upper	0.215	-0.213	-0.512
	lower	1.373	0.735	-0.429
	net	-1.157	-0.949	-0.083
12×12	upper	0.299	-0.127	-0.477
	lower	1.347	0.832	-0.395
	net	-1.048	-0.959	-0.082

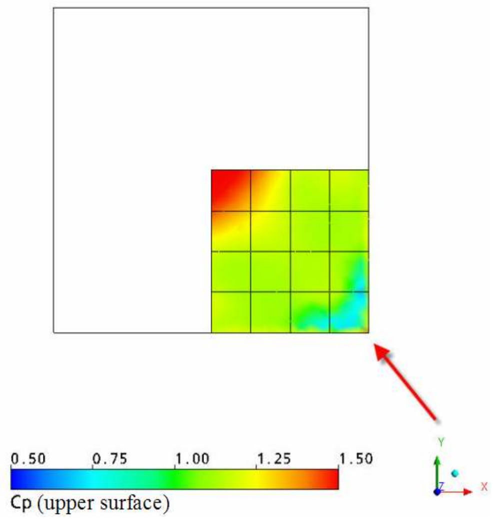

(a) Upper surface

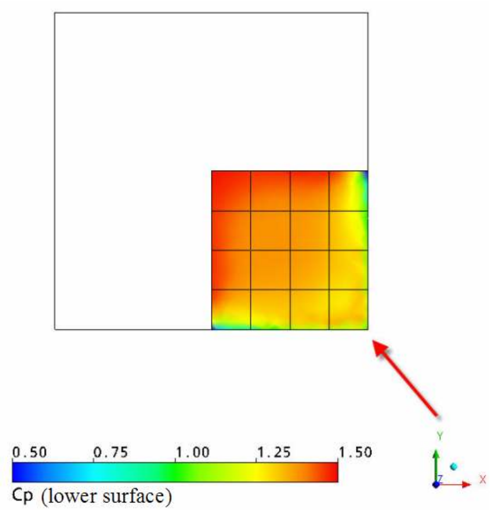

(b) Lower surface

Fig. 8. Cp contour on the upper and lower surface (Canopy size 12 m×12 m).

Table 4. *Cp*, C_f results from numerical simulation for the H/hc=6.

Canopy Size		Wind Direction		
		Front	Side	Rear
3×3	upper	0.969	0.398	-0.578
	lower	0.939	0.402	-0.359
	net	0.030	-0.004	-0.219
6×6	upper	0.976	0.473	-0.436
	lower	0.959	0.494	-0.457
	net	0.017	-0.021	0.020
9×9	upper	0.896	0.459	-0.635
	lower	0.894	0.506	-0.388
	net	0.003	-0.047	-0.247
12×12	upper	0.901	0.387	-0.580
	lower	0.855	0.466	-0.348
	net	0.046	-0.079	-0.231

Table 5. *Cp*, C_f results from numerical simulation for the H/hc=12.

Canopy Size		Wind Direction		
		Front	Side	Rear
3×3	upper	0.848	0.449	-0.485
	lower	0.819	0.440	-0.403
	net	0.029	0.009	-0.082
6×6	upper	1.190	0.438	-0.582
	lower	1.141	0.424	-0.498
	net	0.049	0.014	-0.084
9×9	upper	1.096	0.477	-0.516
	lower	1.021	0.488	-0.302
	net	0.075	-0.011	-0.214
12×12	upper	0.901	0.345	-0.511
	lower	0.838	0.416	-0.307
	net	0.063	-0.071	-0.204

upwards pressure in all canopies except the 12 m×12 m canopy, which had a downward coefficient of -0.8 and an uplift coefficient of +1.1. The net pressure coefficients for the canopies, therefore, lie within the region of approximately 0~0.3. When *H/hc*=6 and 8 in the Table 4 and Table 5, uplift and downwards wind pressure coefficients for all canopies are approximately +1.0, and thus the net pressure coefficients for all canopies are close to zero.

3.2.2 Side wind direction case (arrow 2)

When H/hc=2, the net uplift pressure coefficients of canopies grows steadily from 0.5 through 1.4 as canopy size increases. This is due to the fact that the net uplift pressure coefficient has increased gradually from +0.5 to +1.4 as shown in Table 2 and Fig. 7(b). When H/hc = 4, 6, or 8, the downwards pressure coefficients for upper surfaces of the canopies are shown to be similar for all canopy sizes and H/hc ratios. However, the net uplift pressure coefficients for 3 m×3 m through

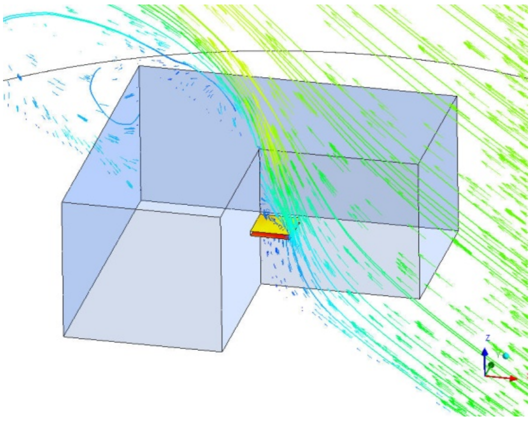

(a) *H/hc*=2

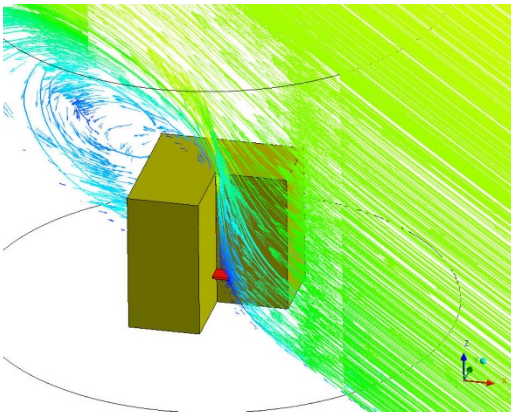

(b) *H/hc*=4

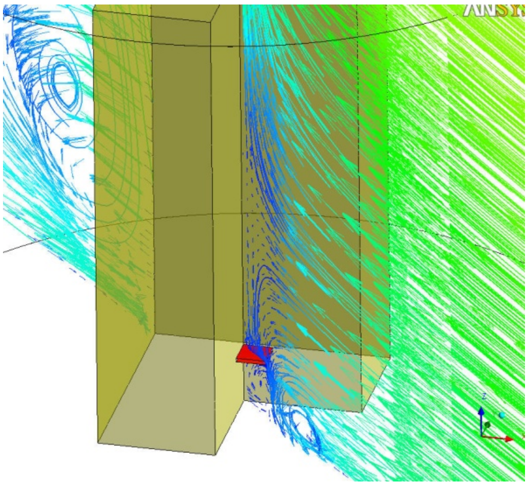

(c) *H/hc*=8

Fig. 9. Velocity vector around the canopy attached building of various heights.

9 m×9 m canopies are shown to be within the range of 0~0.2. Similarly, uplift coefficients lie within the region of 0.5~0.7 for 12 m×12 m canopy.

3.2.3 Rear wind direction case (arrow 3)

The most remarkable feature of rear wind direction is the fact that, in general, canopy size and H/hc ratio have little effect on the pressure coefficients of canopies. Furthermore, the lifting and downwards pressures cancel each other out and the net uplift pressure coefficients lie within the range of 0~0.3 as shown in Table 2 and Fig. 7(c). This wind direction does not have direct impact on the canopy, and also produces the least pressure differences between upper and lower surfaces of canopies as like Fig. 9.

3.3 Effects of wind direction changes

3.3.1 H/hc=2 model case

Our numerical simulation shows that the difference of upper and lower surface pressure coefficients of model canopies is greatest when the wind direction is from the front and this difference is progressively reduced as wind changes to the side and then to the rear direction. In addition, models with H/hc ratio of 2 are found to be most susceptible to pressure variation.

Pressure coefficients for lower surface of canopies are largest when the wind direction is from the front (uplift, +1.4), while they reach +0.4~+0.8 (uplift) for the side and -0.4~-0.5 (downwards) for the rear direction. For upper surface of canopies they are +0.1~+0.4 (downward) front, -0.1~-0.2 (uplift) side and 0.5~-0.6 (upward) for rear wind direction. To surmise, the net pressure coefficients of canopies are 0.1~1.2 (uplift), 0.5~0.9 (uplift) and 0.1~0.2 (uplift) for front, side and rear wind directions respectively.

3.3.2 H/hc=4 model case

Pressure coefficients for lower surface of canopies fall within the range of +1.1~+1.4 (uplift) for front, +0.5~+0.7 (uplift) for side, and -0.4 (downward) for rear wind direction. For upper surface of canopies they reach +0.8~+1.4 (downward) for front, +0.3~+0.4 (downward) for side and -0.5~-0.6 (upward) for rear wind. The net pressure coefficients are 0~0.3 (uplift) for front and 0.1~0.2 (uplift) for side and rear wind directions.

3.3.3 H/hc=6, 8 model cases

Pressure coefficient distribution of 36m and 48m high buildings are very similar to each other.

For lower surface of canopies the pressure coefficients are +0.9~+1.1 (uplift) in case of front wind, +0.4~+0.5 (uplift) for side and -0.4 (downward) for rear wind directions, while for upper surface of canopies they are +0.9~+1 (downward) for front, +0.4~+0.5 (downward) for side and -0.4~-0.6 (upward) for front rear wind. The net pressure coefficients for canopies are 0~-0.1 (uplift) for front and side direction winds, and 0~0.2 (uplift) for rear wind direction.

3.4 Effect of various canopy sizes

Canopy areas ratio used in this simulation is 1 : 4 : 9 : 16. Pressure coefficients vary most with *H/hc*=2 canopies when subjected to side wind. Net pressure coefficients of 3m 6, 9

Table 6. Net pressure coefficients for canopies and awnings attached to buildings (open canopy, wind direction of 0 degree).

Design case	*hc/H* (*H/hc*)	Net pressure coefficients
hc/H<0.5 (*H/hc*>2)	0.1 (10)	1.2, -0.2
	0.2 (5)	0.7, -0.2
	0.5 (2)	0.4, -0.2
hc/H ≥ 0.5 (*H/hc* ≥ 2)	0.5 (2)	0.5, -0.3

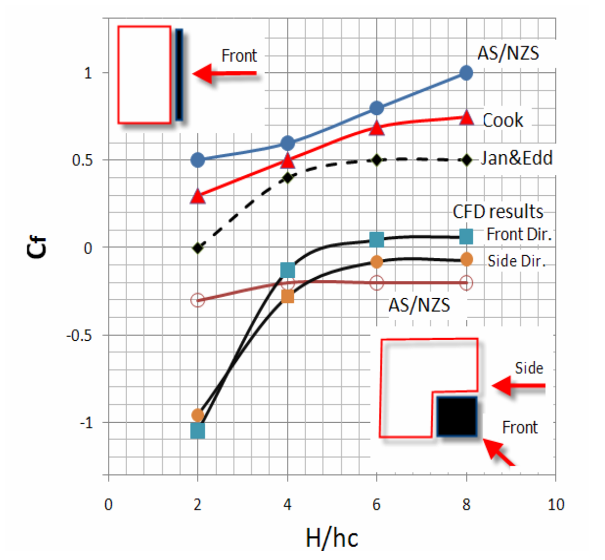

Fig. 10. Various C_f values as a function of *H/hc*.

and 9 m canopies are uplift values of 0.5, 0.7, 0.9 and 0.9 respectively. Net pressure coefficients of canopies with *H/hc*≥4 ratios vary insignificantly for front, side and rear winds regardless of canopy sizes.

Thus, the simulation results shows that canopy sizes have little effect on pressure coefficients of canopies in tall to medium-rise buildings.

3.5 Comparison with codes

The recommendations of Australian/New Zealand Code AS/NZS 1170.2:2002 regarding net wind pressure coefficient on attached canopies of roof slop of 10 degrees or less, are given in Table 6 and Fig. 10. The code recommends that the canopies should be designed for both downward and upward net wind pressure, where indicated. All pressure coefficients should be used with the value of wind speed applying at average roof height.

C_f values in Table 6 are for wind direction normal to the attached wall. For wind parallel to the wall, it is recommended that canopy should be considered as free roof and net pressure coefficients should be obtained accordingly.

Linear interpolation of values in Table 3 gives positive C_f values of 0.5 for the *H/hc* ratio of 2, +0.6 for 4, +0.8 for 6 and +1.0 for the ratio of 8. These values show that pressure coefficients grow gradually as *H/hc* ratios of prismatic shapes increase.

Jancauskas and Eddleston's prismatic wind tunnel test results were linearly interpolated for *H/hc* ratios of 2, 4, 6 and 8, the net pressure of coefficient on canopies were found to be 0, 0.4, 0.5 and 0.5 respectively. These values show that downward pressure coefficients on canopies increase gradually as the value of *H/hc* rises.

Above graph above shows linearly interpolated values of net pressure coefficients on canopies based on Cook's publication (Table 20.28). The publication shows prismatic wind tunnel test results which were then linearly interpolated for *H/hc* ratios of 2, 4, 6 and 8. The net coefficient on canopies was 0 for the *H/hc* ratio of 2, 0.4 for 4, 0.5 for 6 and 0.5 for the ratio of 8.

The graph compares the net pressure coefficients of canopies from this CFD results and other researchers' results. For *H/hc*=2 cases, other researchers who worked with prismatic models returned net pressure coefficients within the range of 0~0.5 (downward) while we returned values in the region of 1.0 (uplift). This shows the effects of L-shaped main building.

Our research shows very clearly that geometry of a building can have profound effects on canopy wind loadings. In cases where *H/hc* is greater than, or equal to 4, net pressure coefficients of our CFD results were markedly smaller than for prismatic model test. Care is thus necessary in the application of the code to buildings of various shapes. For rectangular plan shape buildings, some pressure coefficients can locally exceed the values given in the codes.

4. Conclusions

For the front wind direction case, when *H/hc*=2, the uplift coefficients acting on the lower surface of canopy is dominant and the values lie within the range of +1.35~+1.39, the net pressure coefficient lie within the range of 0.94~1.25. And when *H/hc*=4, the downward pressure acting on upper surface of canopy almost matches the uplift pressure acting on lower surface of canopy, and therefore the net pressure coefficients were negligible for these configurations.

And for the *side wind direction case, w*hen *H/hc*=2, the uplift pressure acting on the lower canopy surface becomes more dominant as canopy size increases, while downward pressure acting on upper canopy surfaces remain fairly constant. Net pressure coefficients, therefore, grow in step with incrising uplift pressures acting on lower canopy surfaces as canopy size rises. And when *H/hc*=4, the *H/hc* ratio and canopy size have little impact on pressure coefficients and net pressure coefficients remain negligible as upward and downward pressures acting on canopies almost cancel each other out.

For the rear wind direction case, *H/hc* ratio and canopy size have negligible effect on pressure coefficients. However, uplift pressure was found to be acting on upper face of canopies, and downward pressure was acting on lower canopy surfaces, showing that the direction of the pressure was opposite to that of the situation comparing with those of *H/hc*=4 cases for side wind. Net pressure coefficients remain negligent as pressures on both sides of the surfaces cancel each other out.

As shown above, numerical simulation results of pressure coefficients on canopies attached to L-shaped models differ greatly from those of previous wind tunnel test results with respect to wind flow directions and wind loadings.

Taking into account the results of numerical analysis, which are based on the effects of building height-to-canopy height ratios, wind directions, and general features of the canopy sizes, it is likely that the wind pressure information generally used by engineers might not be precise enough. That in turn might lead to various complications. Thus, caution is necessary in the application of the Code to buildings of various shapes. For rectangular-based buildings, some pressure coefficients can locally exceed the values given in the Codes. Further wind tunnel tests and research on the subject are necessary in order to obtain accurate characteristics of wind pressure loading on the canopies.

References

[1] L. Jancauskas and J. Holmes, Wind loadings on attached canopies, *Proceeding of the Fifth U.S. National Conference on Wind Engineering*, 3A, 5-2, Texas Tech University, Lubbock, Texas, USA (1985).

[2] M. Paluch, A. Loredo-Souza and J. Blessmann, Wind loads on attached canopies and their effect on the pressure distribution over arch-roof industrial buildings, *Journal of Wind Engineering and Industrial Aerodynamics*, 91 (2003) 975-994.

[3] H. Ueda, H. Hagura and H. Hamada, Wind force on canopies attached to low-rise buildings, *International Conference on Wind Engineering* (1999) 1847-1852.

[4] Y. Uematsu, M. Yamada, A. K., Design wind loads for structural frames of flat long-span roofs: Gust loading factor for a structurally integrated type, *J. of Wind Engineering and Industrial Aerodynamics*, 66 (1997) 155-168.

[5] R. Goyal, A. Ahuja, The distribution of pressure near the corners of flat canopy attached to the gable roof building, *The Fifth International symposium on Computational Wind Engineering (CWE-2006)*, Yokohama, Japan (2006) 127-130.

[6] R. Goyal, A. Ahuja and Prasad, Wind loads on buildings with attached canopies, *Asian Journal of civil engineering*, 8 (3) (2007) 239-246.

[7] K. P. Cho, S. Hong and M. H. Kim, Pressure distribution on canopy of building with different its location, *Jr. of the Wind Engineering Institute of Korea(WEIK)*, (2008) 173-182.

[8] K. P. Cho, S. Hong and M. H. Kim, Evaluation of wind loads on canopy of a building, *Journal of Architectural Institute of Korea(AIK),* (2009) 21-29.

[9] L. Jancauskas and J. D. Eddleston, Wind loads on canopies at the base of tall buildings, *Technical Report No. 31, James Cook University(JCU) Papers at Seventh International Conference on Wind Engineering (ICWE-7),* Aachen, Germany (1987) 12-26.

[10] ANSYS CFX User's Manual, ANSYS CFX Release 11, copyright 1996-2006.

[11] H. R. Kim, S. H. Suh, H. W. Roh, K. Y. Lee and K. S. Kim, Application of computational techniques for studies of wind pressure coefficients around an odd-geometrical building, *Jr. of Wind Engineering and Industrial Aerodynamic,* 67&68 (1997) 659-670.

[12] H. R. Kim, S. H. Suh, H. W. Roh, K. Y. Lee and K. S. Kim, Effects of wind direction changes on the surface pressure of 3-D Model in the boundary layer flow, *Jr. of Wind Eng.*, 63 (1995) 69-70.

[13] AS/NZS 1170.2: 2002, *Australian/ New Zealand Standards, Structural Design Actions, Part 2: Wind actions*, Jointly published by Standards Australia International Ltd., Sydney and Standards New Zealand, Wellington, 89.

[14] N. J. Cook, The designer's guide to wind loading of building structures, *Part2: Static structures* (1990) 472-473.

Hyung-Woon Roh received a Ph.D degree in Mechanical Engineering at Soongsil University in 1999. He has been serving as a CEO for seven years. Currently he is a President of IVAIGD3. He is interested and pursuing an investigation of the small hydropower part, the medical device, the hemodynamic including wind engineering part using the CFD analysis and the experiment.

Ha-Rim Kim received a Ph.D degree in Architectural Engineering at Dongguk University in 1996. He is working as a professor in Architectural Engineering, Juseong University. Nowadays, He is interested in the wind effect on building and structure, codes and regulations.